

Review Article

In vitro three-dimensional cell cultures for bone sarcomas

Javier Munoz-Garcia^{a,b,*,1}, Camille Jubelin^{a,b,c,1}, Aurélie Loussouarn^a, Matisse Goumard^{a,b}, Laurent Griscom^d, Axelle Renodon-Cornière^a, Marie-Françoise Heymann^{a,b}, Dominique Heymann^{a,b,e,*}

^a Université de Nantes, INSERM, Nantes, France^b Institut de Cancérologie de l'Ouest, Tumeur Heterogeneity and Precision Medicine Laboratory, Saint-Herblain, France^c Atlantic Bone Screen, Saint-Herblain, France^d BIOSIT CNRS UMS3480, Université de Rennes-1, Rennes, France^e University of Sheffield, Department of Oncology and Metabolism, Medical School, Sheffield, UK

ARTICLE INFO

Article history:

Received 6 May 2021

Revised 24 June 2021

Accepted 26 June 2021

Available online 6 July 2021

Keywords:

Osteosarcoma

Ewing sarcoma

Chondrosarcoma

Extracellular matrix

3D culture

Multicellular tumour spheroid

Scaffold-based 3D culture

Microfluidics

Bioprinting

ABSTRACT

Bone sarcomas are rare tumour entities that arise from the mesenchyme most of which are highly heterogeneous at the cellular, genetic and epigenetic levels. The three main types are osteosarcoma, Ewing sarcoma, and chondrosarcoma. These oncological entities are characterised by high morbidity and mortality and an absence of significant therapeutic improvement in the last four decades. In the field of oncology, *in vitro* cultures of cancer cells have been extensively used for drug screening unfortunately with limited success. Indeed, despite the massive knowledge acquired from conventional 2D culture methods, scientific community has been challenged by the loss of efficacy of drugs when moved to clinical trials. The recent explosion of new 3D culture methods is paving the way to more relevant *in vitro* models mimicking the *in vivo* tumour environment (e.g. bone structure) with biological responses close to the *in vivo* context. The present review gives a brief overview of the latest advances of the 3D culture methods used for studying primary bone sarcomas.

© 2021 The Author(s). Published by Elsevier GmbH. This is an open access article under the CC BY-NC-ND license (<http://creativecommons.org/licenses/by-nc-nd/4.0/>).

Contents

1. Introduction	2
2. 3D culture methods of primary bone tumours	3
2.1. 3D osteosarcoma culture models	3
2.1.1. 3D culture and drug resistance in osteosarcoma	3
2.1.2. Impact of the tumour microenvironment structure in drug resistance	3
2.1.3. Osteosarcoma cancer stem cells and 3D culture methods	5
2.1.4. Proteomic profile in osteosarcoma 3D cultures	5
2.1.5. 3D osteosarcoma culture as a novel approach to study bone mineralisation	6
2.1.6. 3D culture methods for deciphering osteosarcoma metastatic process	7
2.1.7. Combination of 2D and 3D culture methods for the study of new vessels during osteosarcoma development	7
2.1.8. 3D Ewing sarcoma culture models	7
2.1.9. Drug resistance in 3D Ewing cell cultures	7
2.1.10. Impact of tumour microenvironment in 3D Ewing cultures	7
2.2. 3D chondrosarcoma culture models	8
2.3. 3D models as tool to unravel drug resistance in chondrosarcoma	8
2.3.1. Chondrosarcoma 3D culture approaches to investigate cell adhesion, migration and cell-to-cell interactions	9

* Corresponding authors at: Université de Nantes, Institut de Cancérologie de l'Ouest, Blvd Jacques Monod, 44805 Saint-Herblain, France.

E-mail addresses: javier.munoz@ico.unicancer.fr (J. Munoz-Garcia), dominique.heyman@univ-nantes.fr (D. Heymann).

¹ JMG and CJ contributed equally to the work.

3. Conclusion and future perspectives 9
 Declaration of Competing Interest 10
 References 10

1. Introduction

Bone sarcomas correspond to <0.2% of diagnosed cancers registered in the EUROCARE database and then they are considered as orphan tumours. The three main types of bone sarcomas are: osteosarcoma (OS), Ewing sarcoma (ES) and Chondrosarcoma (CS). Despite their low incidence, bone tumours are associated to high morbidity and mortality, with an important impact in children and young adult population (e.g., 80% of ES patients are under 20 years of age at diagnosis). The absence of specific symptoms at early stages of the disease leads to late diagnosis that frequently corresponds to aggressive phases that include cancer cells spreading and establishment of bone and lung metastases. Unfortunately, whether the 5-year survival rate is 50–70% for OS and ES, there is a drop around 20–30% when lung metastases are detected at the time of the initial diagnostic [1]. CS are associated with high local recurrence associated with high morbidity [2].

OS constitutes the main entity with an incidence of two-thirds of primary bone tumours and affects preferentially children and adolescents. In most of the cases, clinical treatment includes surgical procedure combined with adjuvant and neo-adjuvant poly-chemotherapies with or without radiotherapy. Unfortunately, distant recurrences (with a high predilection for the lung) frequently occur and are associated with drug resistance [2]. OS normally germinates from malignant mesenchymal cells of long bones committed in osteoblastic differentiation and are characterised by the production of an osteoid matrix by tumour cells [3]. The aetiology of the disease is explained by initial somatic mutations of p53, Rb and a BRACness signature that lead to chromosomal instabilities, complex genomic profile and high cellular heterogeneity [2,4]. Cancer stem like cells [5], tumour microenvironment (TME) including immune infiltrated cells and extracellular matrix (ECM) that modulates tumour cell adhesion and migration are also suspected to contribute to this high heterogeneity and to the acquisition of drug resistance [6,7]. Thus, due to their highly complex pathobiology and the limited access to patient samples, a better understanding of OS growth and drug development require the generation of new cell culture methods that mimic native TME of OS [8].

ES is characterized by its high aggressiveness, fatal malignancy developed in bone and extra skeletal sites and with a rapid metastatic expansion mainly in lung. ES is the second most common paediatric bone tumour affecting 3 children per million [9]. ES principally affects Caucasian patients with a slight prevalence in men than women. ES cell classically presents a round morphology, with common expression of the CD99 (MIC2) antigen and chromosomal translocation of the *EWSR1* gene to *ETS* family genes [10]. Experimental evidence suggests that ES cells may originate from undifferentiated mesenchymal stem cells (MSCs) characterised by neuroendocrine features and acquisition of *EWSR1* translocation [11,12]. In addition to conventional chemotherapies, clinical developments are focused on downstream partners of the *EWSR1/FLI1* signalling pathways [13,14]. An important feature of ES is the high resistance to chemotherapy agents, in part due to their particular MSCs origin but also to its complex TME. Reproduction of TME by 3D culture techniques results in a key progress to better understand the behaviour and drug resistance of ES.

CS compose a heterogeneous group of primary malignant tumours characterised by relative low growth ratio and the formation of hyaline cartilaginous neoplastic tissue. Depending on their malignancy, CS are classified in three grades: low-metastatic grade

I, intermediate grade II, and high metastatic grade III [15]. CS are characterised by a high chemo- and radio-resistance mainly due to the presence of large amount of ECM and poor vascularity that restrict the diffusion of anticancer agents and slow down their effectiveness [16]. The importance of these features has motivated the scientific community to switch to 3D culture systems that can reproduce the native CS condition and have the potential to be a great tool for developing new therapies against CS.

Beside the genetic charge present in tumour initiation, TME has emerged as a key factor for tumour development and malignancy. For a better understanding of tumour biology, the scientific community has to reproduce, as close as possible, natural cell growth conditions [17]. During last decades, many technological progresses have been proposed to mimic native tumour biology. Whereas the first documented cell culture methods date from 1885 by Wilhelm Roux [18], the establishment of a true two-dimensional (2D) laboratory tissue culture system has been described by Ross Harrison at the beginning of the 20th century [19]. This event led to a scientific revolution in the understanding of cell behaviour during healthy and pathogenic situations. While 2D cell culture techniques became standards in research laboratories for a wide window of studies and fields, they do not reproduce the dynamic evolution of tumour growth and failed to mimic cell-to-cell or cell-to-microenvironment interactions. To overcome these 2D culture issues, during last decades, a variety of 3D cell culture techniques has been developed including liquid-based scaffold free methods, scaffold 3D systems and the emerging organ-on-a-chip platforms: microfluidics and bioprinting systems [20–23].

Briefly, liquid-based scaffold-free methods are based on the prevention of cell adhesion to the cell culture container surfaces (e.g., vessels, plates) by coating them with non-adherent materials such as agar or poly-hydroxyethyl methacrylate [24]. The absence of adherent surfaces promotes cell-to-cell adhesion and formation of spontaneous spheroids. Wide variety of low/non-adherent supports are commercially available nowadays. Hanging drop technique is another liquid-based scaffold free methods that allows the production of spheroids using mono- or multi-cellular (co-cultures) approach thanks to the effect of the gravity (Fig. 1) [25,26]. Low adherent supports and hanging drop methods have been also widely used to study cell organisation, embryonic development, tumour biology and tissue formation [25,27–32]. However, one of the main drawbacks of liquid-based scaffold methods is the lower reproducibility and control of the surrounding cell microenvironment.

Scaffold 3D systems consist in a structural support that favours cell adhesion, proliferation, migration, cell-to-cell interaction and signalling [33,34]. Natural scaffolds are based on molecules that are present in the ECM such as collagen, gelatine and derivatives [35,36], complex matrix (e.g., commercial Matrigel™) and hydrogels [37,38], and polysaccharides as alginate, chitosan or hyaluronic acid [39–43]. Whereas the main advantage of these natural scaffolds is their biocompatibility, their production and inter-batches variability are the main issues of these materials. To solve these problems, synthetic scaffolds characterised by high stability, reproducibility and biocompatibility have been developed [44]. The most used synthetic scaffolds are based on polyethylene glycol (PEG) polymer hydrogels [45–48].

Finally, organ-on-a-chip platforms are based on microfluidic devices or 3D bio-printed systems [49–53]. Both techniques allow

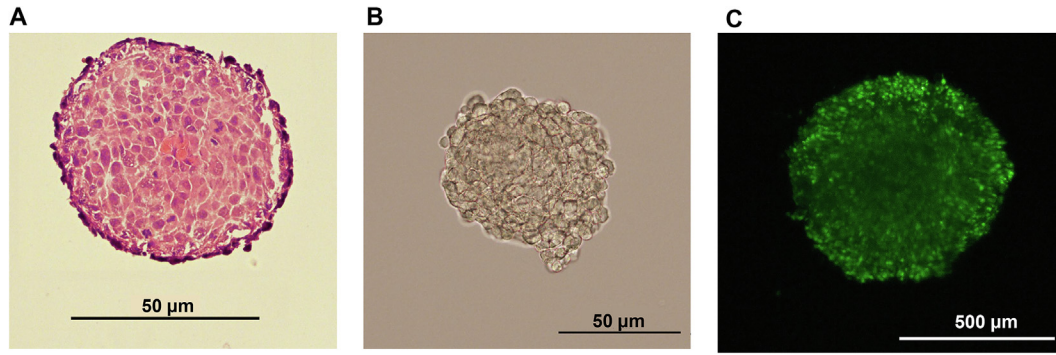


Fig. 1. Osteosarcoma spheroid. Representative images of OS spheroid. A) HES staining of MNNG/HOS spheroid. B) Wide-field MNNG/HOS spheroid using a Nikon Eclipse Ni microscope. C) MNNG/HOS spheroid at day 3 obtained from 20,000 cells in DMEM (Gibco®) supplemented with 1% L-glutamine plus 10% FVS using 96-well low adherent plate U-bottom (ThermoFisher), labelled with Vybrant™ DiO (ThermoFisher) and imaged in a Operetta CLS high-content analysis system (PerkinElmer).

a precise control of the TME by applying a tuneable perfusion of media that mimics blood flow and facilitates a continuous access of nutrients, oxygen and drugs [54–56]. In addition, these systems can reproduce the complexity of tissue by adding layers or compartments by co-culture of different various sets of cells in the presence of various ECM components [57–59].

In the present review, we will focus on the different 3D culture techniques recently developed for the three main bone sarcoma entities.

2. 3D culture methods of primary bone tumours

2.1. 3D osteosarcoma culture models

With a low 5-years survival rate and no improvement in the last 4 decades, OS is a rare and devastating oncological entity that affects mainly children and young adults. The complexity of the bone structure and surrounding TME imply that 2D monolayer culture stays far away from the organisation of natural tumour tissue and impairs the study OS development [7].

2.1.1. 3D culture and drug resistance in osteosarcoma

Low attachment and hanging-drop cell culture are the most frequently employed liquid-based scaffold-free method [60] and consist in an easy 3D approach for generation of OS spheroids to study cell behaviour and drug resistance (Fig. 1 and Fig. 2) (Table 1). By using hanging-drop methodology, Rimann *et al.* demonstrated that spheroids produced from established cell lines, like SaOS2 or HOS, exhibited a totally different pattern of resistance to a panel of anti-tumor drugs compared to 2D (monolayer) culture methods [61]. Indeed, the IC50 values for doxorubicin, cisplatin, taxol, and taurolidine significantly increase in 3D culture, meaning that 3D cells are more resistant to those drugs than monolayer culture. Those data were consistent with the observation done in patients where treatment based in 2D dose concentrations showed a decrease of drug effectiveness compared to 2D culture [61]. Many papers appeared reinforcing the concept that 3D spheroids are really closed to real tumour behaviour to drug treatment [61–65]. Similarly, U2OS spheroids generated by ultra-low attachment methods were used to mimic tumour structures and demonstrated the potential use of the nuclear NAD synthesis enzyme nicotinamide mononucleotide adenylyltransferase-1 (NMNAT1) as a target for anti-tumour drugs [66]. The expression of this enzyme increased in several tumour cell lines after exposure to DNA damaging agents as cisplatin and doxorubicin, suggesting an important role of this enzyme in tumour resistance [66].

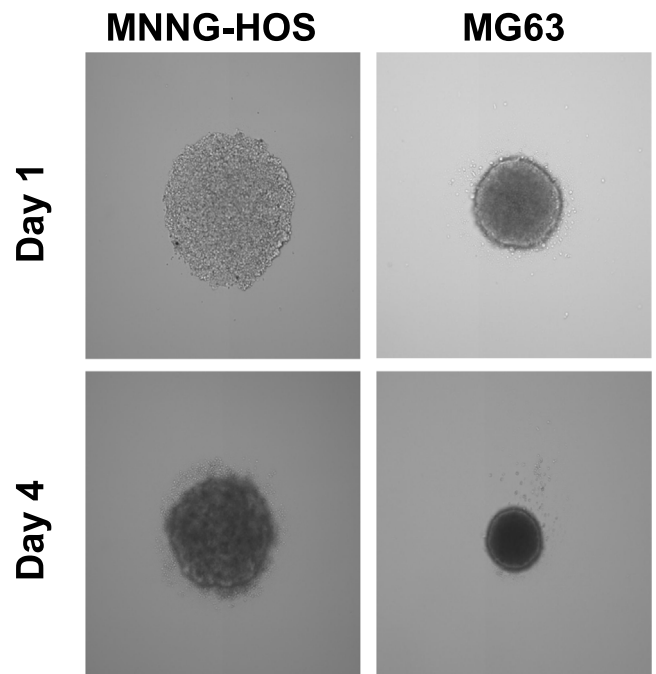


Fig. 2. Sarcospheres from different OS cell lines. Representative images of OS spheroid formed from different OS cell lines depicting differences in size and morphology. MNNG-HOS and MG63 OS cells were plated at 5,000 cells/well and 2,500 cell/well respectively in low adhesion plates (Corning Costar®) coated with DMEM (Gibco®) + 10% agarose and imaged on days 1– 4 using the Celigo Imaging Cytometry System (Nexcelom Bioscience).

2.1.2. Impact of the tumour microenvironment structure in drug resistance

Cancer cells receive multiple signals (autocrine, juxtacrine and endocrine messages) coming from their cellular neighbours, the extracellular matrix and distant organs. By integrating all of the information, cancer cells change their behaviour, modify their metabolism and migration properties and become quiescent, or highly proliferative or resistant to drugs. TME then plays a crucial role in drug resistance [67]. Whereas hanging drop techniques have been used with success for rapidly forming tumour spheroids, this approach is far from wholly reproducing the natural TME controlling the cancer cell behaviour. 3D cell culture based on scaffold methods using natural components identified in the natural TME is one of the strategies proposed to mimic the environment of cancer cells. Interestingly, 3D scaffold are also bivalent tools not only

Table 1
3D methods used in primary bone tumors.

Bone tumor	Technique	Material	Cell line	Reference	
Osteosarcoma	Scaffold-free	Hanging drop and Low-attachment	SaOS2	61–66,83,84,86,109	
			HOS		
	Scaffold	Algininate beads	U2OS	68,72,78,83	
			D17		
			MG63		
			Silk sponge	LM8	69
				MG63	
			PEG	SaOS2	71
				HOS	
			Collagen	SaOS2	72,74,76,90–94,110
				MG63	
			Agarose	U2OS	72
				MG63	
			PCL	MG63	73,102
				HOS	
Methylcellulose	HOS	77			
	MG63				
PLA	MG63	97			
	MG63				
HA	MG63	84,85,102,107			
	OS MSC				
BCP	OS MSC	101,107			
	SaOS2				
Complex matrix	SaOS2	70,72,84,92			
	U2OS				
Ewing Sarcoma	Microfluidic/Bioprinting	PDMS	MG63	96,110 98,99,106–109	
			SaOS2		
			RD-ES		
Ewing Sarcoma	Scaffold-free	Hanging drop and Low attachment	A673	112,117–119	
			SK-N-MC		
			VH-64		
			T-32		
			TC-71		
	Scaffold	PCL	A4573	111,113,114 115	
			TC-71		
			RD-ES		
			A673		
			SK-N-MC		
Ewing Sarcoma	Scaffold	HA	RD-ES	115	
			A763		
			SK-N-MC		
			A673		
			Agar		
Chondrosarcoma	Scaffold-free	Algininate Hanging drop and Low attachment	Primary cell lines	120 121,122 127–131,133	
			SW1353		
			CAL78		
			OUMS27		
			CH03		
	Scaffold	Levitation forces Algininate	CH34	140 134,135	
			CH56		
			CH2879		
			L835		
			SW1353		
Scaffold	Collagen Titanium beads	CH28979	136,138 137		
		JJ012			
		SW1353			

PEG: polyethylene glycol; PCL: poly(ϵ -caprolactone); PLA: poly(D,L-lactic acid); HA: Hydroxyapatite; BCP: biphasic calcium phosphate; PDMS: Polydimethylsiloxane

usable in *in vitro* assays but also as support of cancer cells in *in vivo* animal experiments. The use of alginate beads is a perfect example of a 3D scaffold frequently applied to the oncology field. Alginate is used firstly to encapsulate and proliferate OS cells in a 3D spheroid configuration, and secondly for studying the metastatic effect of OS cells in animal model after inoculation of encapsulated cells [68]. The drug sensitivity was compared between 2D and 3D cell culture conditions and revealed a significant higher drug resistance when cells were cultured in 3D scaffolds compared to monolayer (2D) cell cultures. The use of silk sponges was also described as 3D scaffold for the expansion of SaOS2 and U2OS cell lines, which appeared less sensitive to drug treatment (doxorubicin and cisplatin) than cell lines cultured in a 2D environment [69]. 3D SaOS2 and U2OS cell spheroids were also generated by using commercial

culture plates coated with various matrix: hyaluronic acid, collagen and adhesion proteins (Biomimesys™ matrix, from HCS Pharma, France). By using such an approach, 3D cultures differentially modulated the ATP binding cassette transporter A1 (ABCA1) and B1 (ABCB1, also known as Multidrug resistance protein-1, MDR1) expressions associated with the drug efflux and resistance which has not been observed in 2D environments [70]. 3D culture cells exposed to doxorubicin were characterised by a higher expression of ABCB1 implicated in the intracellular drug efflux, induced by the ERK1/2/HIF-1 pathway. Surprisingly, the increase of expression of ABCB1 was accompanied by a reduction of ABCA1 and by T-cell inactivation. ABCA1/ABCB1 ratio was then related to the chemo- and immune sensitivity of human OS. These resistances were reversed when ABCA1/ABCB1 ratio was increased

[70]. This observation suggested that the upregulation of ABCB1 transporter may induce an anti-drug and anti-immune resistance properties in OS tumours.

The physical characteristics (e.g. elasticity) of the scaffolds influence cancer cell properties. The generation of a hydrogel with a tuneable network of PEGDA and Gelatin-Methacryloyl (GelMA) enabled the control of the stiffness and adhesion properties of the substrate. The stiffness of the substrate correlated with the proliferation and progression of SaOS2 OS cells which proliferated much better when the rigidity of the substrate increased. This stiffness dependency relied in the regulation of the integrin-mediated focal adhesion signalling pathway [71]. Similarly, a recent study compared the viability of OS MG63 cells cultured in four different scaffolds (collagen, Matrigel™, alginate and agarose) and demonstrated that their viability was also dependent on the scaffold elasticity [72]. Whereas cell adherence was similar for the different cell types in 2D models, ranking collagen as the best substrate followed by Matrigel™, alginate and agarose, 3D cultures of OS cells were more dependent on substrate elasticity for an optimal proliferation. In this case, robust gels such as collagen and agarose are more proliferative substrates than softer hydrogels, Matrigel™ and alginate. Interestingly, even if the four substrates were able to produce *in vivo* tumour in animal model, tumour size and angiogenesis process also correlated to the elasticity of the substrate and showed higher size and micro-vessel formation in collagen and agarose than in Matrigel™ or alginate [72]. Mechanical properties of the ECM were also related to the drug resistance of cancer cells. Molina *et al.* developed a 3D culture system that allows mechanical modulation of TME by changing substrate stiffness [73]. They observed that lower stiffness induced the nuclear localisation of mechanotransduction pathways, contributing to specific drug resistance to anti insulin-like growth factor-1 and mTOR drugs [73]. By using collagen scaffold, Fallica *et al.* demonstrated that U2OS osteosarcoma cells exhibited increased resistance to the anti-proliferative drug PI103 in 3D gels than in conventional 2D cultures [74]. These authors observed that the increase of collagen concentrations augmented the resistance of OS cells to the inhibitor. This observation was in agreement with many clinical cases in which the increase of collagen levels in TME was associated to a poor patient survival [75]. Reinforcing the importance of collagen scaffold composition, Charoen *et al.* demonstrated that concentration of 3–4 mg/ml of type I-collagen gels was crucial for optimum development of OS spheroids, whereas the optimum concentration for MDA-MB-231 breast cancer spheroids was 2 mg/ml [76]. These data suggest that production of specific tumour niches depends on tissue ECM composition. Matrigel™ or agarose were replaced by methylcellulose for facilitating the development of cancer cell spheroids. Based in an *in vitro* methylcellulose scaffold model, Bai *et al.* generated spheroids from HOS1 OS cell line and various soft-tissue sarcomas including HT1080 fibrosarcoma, RD rhabdosarcoma, SW872 liposarcoma cells. Spheroids formed in this 3D environment showed more resistant properties to doxorubicin, gemcitabine and docetaxel or X-ray radiation than those formed in 2D cultures [77].

Tumours are characterized by a high heterogeneity of cell distribution with a necrotic or apoptotic core surrounded by quiescent layer of cells followed by proliferative cells. This tumour stratification is associated with a different TME composition in each tumour region. The determination by mass spectrometry imaging (MSI) of the spatial distribution of metabolites in response to doxorubicin treatment on SaOS2 OS cells cultured in alginate compared to 2D underlined the role of the 3D environment. The combination of 3D culture and MSI techniques represent a new tool to better understand drug activities and design new therapeutic approaches [78]. In addition to its role in anti-tumour drug resistance, TME plays a role in cell accessibility for genetic manipulation. 3D min-

eralized alginate-chitosan cell encapsulation resulted in an efficient tool for gene transfection in human bone cells [79]. Polysaccharide beads facilitated gene uptake by SaOS2 cells when specific calcium phosphate and chitosan rate were used indicating that microcapsule environment composition is crucial for gene transfection in 3D bone model [79].

2.1.3. Osteosarcoma cancer stem cells and 3D culture methods

OS, and other tumours, are composed by highly heterogeneous cell populations that include “Cancer Stem Cells” (CSCs) or “tumour-initiating cells” [6,81,81]. CSCs combine stem cell features with tumour characteristics as tumour initiation ability, dormancy, recurrence and metastasis [79,82]. Thus, CSCs respond differently to anti-tumour treatments than non-CSCs tumour cells by showing a more resistant drug phenotype and leading the role of treatment failure [81]. CD133 CSC spheroids were generated from the SaOS2 cell line by using a scaffold-free 3D model based [83]. The generated spheroids were viable, conserved their pluripotency, and constituted an ideal model for drug screening. CSCs enrichment from MG-63 and SaOS2 spheroids by scaffold-free method was combined with two hybrid scaffolds that mimic ECM and used to analyse the impact of ECM in OS CSCs development [84]. Hybrid scaffold was constituted by Mg-doped hydroxyapatite coupled to collagen fibres and a porous hydroxyapatite substrate. Both hybrids scaffolds resulted in stable CSCs enriched OS spheroid growth without any loss of round morphology compared to 2D. Moreover, an increase of stemness markers including OCT-4, NANOG and SOX-2 was observed that indicated that both types of hybrids scaffolds were able to mimic native environment promoting CSC stimulation [84]. Hydroxyapatite nanoparticle 3D cultures had a strong impact on the survival of OS cells under anti-tumoral oxidative stress therapy [85]. Cold atmospheric plasma resulted in a potential therapy in OS by induction of oxidative stress and subsequently cell death in 2D cultures. However, when this therapy was tested in 3D, MG-63 OS cell cultures in hydroxyapatite nanoparticles were characterised by a significant decrease of cell death [85]. This property was related to 3D environment due to the nanoparticles that favoured cell scavenging and evasion from reactive oxygen and nitrogen particles. Moreover, the generated 3D TME enhanced CSCs subpopulation expansion [85]. These data suggest a relevant role of TME in the development and drug resistance of CSC on OS, and the advantage of the use of 3D culture techniques that mimic native 3D OS nature unlike 2D approaches.

2.1.4. Proteomic profile in osteosarcoma 3D cultures

Protein expression and modification are highly impacted by nutrient availability and TME. Interestingly, the protein expression profiles significantly differ between 2D and 3D cultures. A proteomic study using spheroids produced by ultra-low attachment supports from the dog OS cell line D17 demonstrated that the development in 3D culture induces an increase of glycolysis/gluconeogenesis pathways, biosynthesis of amino acids and changes in carbohydrate metabolism [86]. These data were in agreement with the metabolism observed during tumour development and the generation of a hypoxic local environment. Chaperon's family, which is composed by protein folders associated to cellular stress response and cytoskeletal organization, is similarly modulated by 3D context. On the opposite manner, general protein phosphorylation is upregulated in 2D cultures compared to 3D environment, probably due to the increase in the growth rate observed in monolayer cell cultures [86]. These data suggest that, in order to better understand the proteomic profiles presented in tumours, all the previous information obtained by 2D studies must be re-evaluated in the light of the 3D culture methods close to the tumour behaviour.

2.1.5. 3D osteosarcoma culture as a novel approach to study bone mineralisation

OS is characterised by the production of mineralised tissue. Osteoblastic-like OS cells show an increase in the level of protein implicated in the mineralisation process (as TNAP, BMP-2 and CaSR). The faster osteogenic properties of OS cells make them an interesting tool to better understand the bone mineralisation process. While 3D culture techniques have been widely developed for mimicking TME and, subsequently, more reliable anti-cancer drugs screening, bone 3D cultures were also used to study osteogenesis biology.

Natural and synthetic scaffold gels generate a macro- and microstructural configuration similar to the trabecular bone identifying these materials as perfect supports to study bone mineralisation [86–89]. Type I collagen stands out as a great 3D scaffold for bone mineralisation in which SaOS2 cells can be expanded. Magnesium is a key cation involved in many biological activities such as metabolism, muscle contraction and bone cell function. Almost 50% of the magnesium present in the body is associated with bone tissue (hydroxyapatite crystals, HA) and influences bone-remodelling processes. By using a 3D collagen scaffold approach, Picone *et al.* showed that intracellular magnesium was incorporated at the early phase of bio-mineralisation, a process which may favour HA platelet formation and interfibrillar mineralisation [90]. The composition of culture media appeared critical similarly to the 3D environment. Indeed, a Modified Eagle's Medium resulted in a better mineralisation induced by SaOS2 that conventional medias (e.g. Dulbecco's Modified Eagle's Medium) used for this cell line [91].

The morphology of mineralised matrix produced by HOS OS cells strongly differed according to the cell culture condition used (2D to 3D) [92]. While 2D cell cultures produced spheroid particles in the surrounding cell layers, in 3D culture conditions (type I collagen and poly-ion complex hydrogels) amorphous mineralised particles were observed at the matrix layers. This phenomenon produced gel turbidity that could be used as an indicator of the level of mineralisation [92–95]. These data indicate that 3D gels are interesting approaches for osteogenesis studies associated with OS development. However, structure and mechanical properties of 3D gels are crucial parameters for investigating bone mineralisation. Similarly to tumour development, the pore size of the matrix used to promote osteogenesis is a critical factor. Using bioprinting approach, Vanderburgh *et al.* showed that a 300 μm pore size produced the optimum osteoblast differentiation and mineralisation. In addition, this pore size also favoured OS tumour growth and proliferation [96]. The distribution of pores also influences the structure of the extracellular matrix. The comparison of two types of 3D poly(D,L-lactic acid) scaffolds, one with regular pore distribution and the other with random distribution, showed that both types were adapted substrates for the attachment and proliferation of MG63 OS-derived osteoblasts. However, the random pattern, which is closer to real bone structure, induced a better distribution and organization of collagen fibres [97]. Polydimethylsiloxane (PDMS) is widely used as material to produce microfluidic devices but it can be also used as a scaffold for cell cultures [98]. A water-PDMS emulsion was used as a porous template for SaOS2 OS proliferation. Playing with different curing parameters for PDMS and pressure, Riesco *et al.* generated various grades of PDMS reticulation that allowed proper adhesion and proliferation of OS cells. Moreover, this system provides a fast and cheap way to produce scaffolds in mass [98]. As mentioned before, PDMS is the most commonly used material for microfluidic device fabrication (Fig. 3). A microfluidic chip was developed for the production of OS spheroids in mass (up to 5000) [99]. Microfluidic device was treated with a surfactant (Synperonic®) to generate a non-adherent surface that favoured the generation of MG63 spheroids



Fig. 3. 3D Spheroid PDMS chip. PDMS microsystem for spheroid cell culture in a 60×22 mm slide. Microsystem is constituted by a reservoir for media (a 15 ml Falcon tube cut at desired size) glued to the PDMS microsystem. The reservoir is connected to the cell culture chamber by an 8 mm length channel (200 μm wide and 70 μm high). Cell culture chamber is 4 mm wide by 20 mm long (height 200 μm). To slowdown media flow, a 2 cm long serpentine channel (200 μm wide 70 μm high) was placed after the cell chamber. Output through 1.5 mm Tygon tubing with 500 μm internal diameter.

in a similar way as non-adherent plates. Massive production of spheroids was used to challenge spheroids to two different cellular stresses: nutrient deprivation (serum concentration) and hypoxia (HIF inhibition). 3D cultures obtained data confirmed *in vivo* observation where stress conditions favoured the increase of VEGF secretion and induction of malignancy processes [99]. This study confirmed the impact of ECM variation in tumour malignancy as well as demonstrated that microfluidic approaches represent an interesting tool for massive 3D cultures and analysis. However, it has been reported that the combination of commercial OS tumour cell lines and collagen and Matrigel™ scaffolds may not be the perfect model for 3D tissue bone engineering studies [100]. The hypoxia observed in 3D cultures using scaffolds like collagen and Matrigel™ generated less oxidative stress by tumour cells than in 2D. In addition, this oxidation can negatively impact the bone mineralisation [100]. By using non-tumour cell lines, Gamblin *et al.* generated 3D cultures to study osteoblastic and osteoclastic differentiation [101]. Based on biphasic calcium phosphate microbeads scaffolds, these authors induced the proliferation of MSCs that adhered and proliferated with abundant production of collagenous ECM. Interestingly, the system promoted the co-cultures of differentiated MSCs with osteoclasts generated from peripheral blood CD14-positive monocytes. Altogether, the system was able to mimic bone precursors behaviour and established a valid non-tumour approach to study drugs for bone healing, osteoporosis and OS biology [101]. The production of hybrid scaffolds as the combination of layers of biodegradable polymer poly(ϵ -caprolactone) (PCL) and layers of chitosan in combination with HA by electrospinning method resulted in continuous micro- and nano-fibers with high surface area and micropores that provided optimal attachment and proliferation of SaOS2 OS cells with high mineralisation activity [102]. Bioprinting methods have been also used to produce hybrid hydroxyapatite-chitosan-genipin hydrogels to analyse nanomechanical properties of generated bone tissue [103]. Bioprinter hybrid scaffolds resulted in a good structured TME that favoured 3D MG63 OS cell adhesion, culture and proliferation [103], indicating that bioprinting methods constitute interesting platforms to analyse how the composition and architecture of ECM impact bone mineralisation.

Other types of scaffold methods for 3D culture of OS cells imply the use of stirred-tank bioreactors [104]. Based on this equipment, Chen *et al.* developed a fibrous bed bioreactor with a 3D polyester

fibrous matrix that resulted in a better production of 143B OS spheroids compared to 2D cell cultures. Moreover, they gave evidence that a 3D scaffold favoured the retention of viable and non-apoptotic tumour cells together with a long-term stability [104].

2.1.6. 3D culture methods for deciphering osteosarcoma metastatic process

OS cells are characterized by their ability to spread to distant tissues forming metastases (lung and bone) as carcinomas. To understand the process of cell dissemination and metastasis development, 3D bone tissue cultures were produced using a microfluidics device to mimic and analyse the “metastatic” installation in bone [105]. Hao *et al.* [106] developed a bone-on-a-chip microfluidic device in which they generated mature osteoblastic tissue using the MC3T3osteoblast precursors cell line. Cells produced a layer of heavily mineralised collagen fibres up to 85 μm in thickness. By using this system, they analysed similarly the capability of metastatic breast cancer cell line (MDA-MB-231) to invade bone tissue. After 14 days of co-culture, cancer cells seeded and invaded the apical layer of mineralised bone tissue in an “Indian file” and formed “micro-metastases” [106]. Choudhary *et al.* developed an interesting microfluidic PDMS device that contained culture chambers in which primary human osteocytes were cultured in the presence of collagen-coated biphasic calcium phosphate microbeads for producing bone tissue in hypoxic conditions. Co-culture of conditional reprogrammed prostate cancer cell line (PCa3) with 3D osteocyte culture induced an increase of fibroblast growth factor-23, RANKL mRNA expression levels and alkaline phosphate activity by osteocytes that was associated to an increase of the mineralisation process. These results suggested that 3D microfluidic devices can be useful to better understand the metastatic process induced by primary tumours in bone tissue [107]. 3D microfluidic devices were also used to analyse the cell traction force in confined TME [108]. This device consisted in deflectable PDMS microspots included in micro-channels with different wide cross-sections. Migration test using HOS OS cells demonstrated that, in contrast to what observed in non-confining microchannels, tumour cell traction forces did not depend on myosin-II. This result showed that migration mechanisms of tumour cells during metastasis can vary depending on tissue structure, which compromises anti-metastatic drug approaches. Moreover, the traction force devices resulted in an appealing approach for new anti-metastatic drug selection screening [108].

2.1.7. Combination of 2D and 3D culture methods for the study of new vessels during osteosarcoma development

An alternative to the development of complex 3D micro systems is the combination of 2D and 3D cultures. To study angiogenesis process during tumour development, 3D MG-63 OS spheroids were generated by hanging drops using Gravity PLUS plates, reaching a size of 400 μm in diameter, and co-cultured with a HUVEC endothelial monolayer [109]. MG-63 OS spheroids produced similar ECM compared to *in vivo* tumours and acquired similar tumour architecture with proliferation cells at the periphery and quiescent cells at the centre of the spheroids. The generation of a hypoxia compartment induced the production of VEGF factor by tumour cells promoting proliferation and differentiation of HUVEC to produce vascular tubule-like structures. Using dog OS cell lines (D22 and D17) and 3D collagen gels, Massimini *et al.* demonstrated that a non-human OS model was associated with induced vasculogenic mimicry and that 17-AAg drug abolished tumour progression and micro vascular channel formation [110].

2.1.8. 3D Ewing sarcoma culture models

ES is the second most common paediatric bone malignancy and the third most frequent primary bone sarcoma after OS and CS. In addition to the *EWS/ETS* fusion gene which is at the origin of the disease, numerous investigations highlighted the contribution of the TME in the progression and malignancy of ES [111]. Similarly to OS, scientific community has put their effort to set up new *in vitro* ES models (Table 1).

2.1.9. Drug resistance in 3D Ewing cell cultures

Electrospun polymeric scaffolds based on the inert polymer PCL have become a promising 3D platform to study mechanistic and drug resistance processes in TC-71 ES cell line. TC-71 3D culture reproduced morphology, proliferation and protein expression similar to observations in human tumours. As remarked in OS models, a 3D configuration induces more resistance to drug treatment (doxorubicin) than 2D cultures [110,112]. Interestingly, the PCL 3D model revealed that the IGF-1R/mTOR signalling pathways were highly activated in ES 3D models and these pathways played a key role in the upmodulation of tumour cell adhesion, identifying IGF-1R/mTOR signalling pathways as new potential targets for drug treatment in ES [111]. Similarly, Santoro *et al.* emphasized the role of IGF1/IGF-1R pathway and biomechanical TME stimulation in drug resistance by using similar 3D models [113]. These data are in agreement with the recent study published by Molina *et al.* [114]. Indeed, these authors demonstrated that 3D TME favoured the downregulation of IGF-1R via mTOR pathway, which was accompanied by a reduction of the clathrin-dependent nuclear localisation and transcription activity of IGF-1R [114]. TC-71 3D culture was exposed to different shear stresses close to those observed in bone microenvironment in a flow perfusion bioreactor. Under shear stress, 3D ES cells enhanced cell tumour proliferation and induced an increase of IGF1 pathway compared to 2D cultures. Besides, the increase of IGF1 levels was associated to the resistance to dalotuzumab (an inhibitor of IGF1 receptor) and the downregulation of the c-KIT and HER2 oncoproteins [113]. These data suggested that biomechanical forces impacted the progression and malignancy of ES cells [113]. When ES spheroids were grown in a 3D mimic bone tissue, there was an increase in ERK1/2 phosphorylation and RUNX2 protein levels associated to drug resistance that was not observed when the same cells were cultured in 2D [115]. Interestingly, an increase of RUNX2 level was similarly observed in patients suffering from ES [115]. All those data suggest that ECM displays a key role in ES drug resistance by induction of specific mechanotransduction signalling pathways including RUNX2.

2.1.10. Impact of tumour microenvironment in 3D Ewing cultures

ES are characterised by a rapid development of multidrug resistance due to the overexpression of Multidrug resistance associated protein-1 (MRP1) and ABCB1 [116]. Similarly to OS, the drug resistance of ES cells was also related to a set of stem cells with tumour-initiating properties with a development dependent of TME [116]. Supporting this idea, ES spheroids produced by ultra-low attachment method under serum-free conditions failed to generate tumour-initiating cells [117]. Although ES cells (VH-64, TC-32, TC-71 and A4573) form spheroids in serum-free media with a diameter ratio of 200 μm and with phenotypes similar to 2D cultures, none of them was able to self-renew or expand in a clonogenic manner indicating that TME is a key factor for ES enrichment [117]. Reinforcing the role of TME in ES development, Villasante *et al.* developed an interesting 3D model based on the combination of an engineered bone tissue with spheroids produced from different ES cell types (RD-ES, SK-N-MC and EWS-GFP) [118]. Bone tissue was generated from induced osteogenic differentiation of human MSCs in a native bone ECM, whereas ES spheroids were formed thank to the intrinsic nature of ES cells to generate cell

aggregates after long period of culture (one week at 37 °C in Eagle's Minimum Essential Medium supplemented with 10% Hyclone FBV [119]). The co-culture of these ES spheroids in the tissue bone matrix recapitulated the tumour behaviour, including the re-expression of focal adhesion and related cancer genes, generation of a hypoxic and glycolytic phenotypes and development of angiogenesis potential [118]. This study pointed out the requirement of specific niche configuration for proper development of ES. Reproduction of hypoxic conditions is indeed necessary to better understand how tumours develop angiogenic mechanism. Agar coated plates were used to induce A673 ES spheroids that were moved to a hypoxia chamber for analysing the functional relationship between hypoxia, spheroid cell distribution and DNA damage response [120]. Under hypoxic conditions, A673 ES spheroids displayed a stratification of cellular population from necrotic cells at the nucleus of the spheroids to proliferating cells located at their surface. Moreover, cells localized at the nuclear and perinuclear zone of the spheroids were characterised by an increase of γ -H2AX via the ATM DNA repair pathway, indicating that this approach can be used for anti-ATM drug development in ES [120]. Recently, a new approach was described for encapsulation in alginate spheres of ES cells isolated from patient derived xenografts without losing their phenotype [121]. While ES primary cultures were maintained for at least one month, cells at the core of spheroids did not undergo to hypoxia which is a key step of tumour angiogenesis. That could be due to the limitations in spheroid size by the alginate beads tested (<200 μ m), as hypoxia has been observed when spheroids reach a size over 400 μ m [122]. Overall, this method has an interesting potential as drug screening platform and can be easily implemented for hypoxia studies. In addition, encapsulation of different cell types in alginate beads can be a useful tool for cell-to-cell interactions in ES.

2.2. 3D chondrosarcoma culture models

CS is the second most frequent bone cancer characterised by the production of malignant cartilaginous matrix [122,124]. Surgery is the only effective medical treatment as CS are characterised by a high resistance to chemo- and radiotherapy. However, the mechanisms that control and regulate CS differentiation are still not well defined. MSCs can undergo into chondrogenic differentiation and have been used to understand the gene expression that determine 3D chondrogenic mechanism [125]. Chondrogenic differentiation of MSCs was associated to an increase of *SERPINA1* and *SERPINA3* mRNA expression. Moreover, secretion of *SERPINA-1* correlated with chondrogenesis and dedifferentiation during chondrocyte expansion, suggesting that *SERPINA1* could be considered as a marker of chondrocyte differentiation [125]. Similarly, MSCs were used for studying chondrocyte differentiation in spheroids and simultaneous gene expression profiles to determine genes implied in pre-chondrogenic and chondrogenic phenotype compared to tumour samples [126]. Comparative gene analyses allowed the identification of two clusters that mainly include ECM components, remodelling matrix enzymes and few growth factors useful to predict the clinical behaviour of CS subtypes [126].

2.3. 3D models as tool to unravel drug resistance in chondrosarcoma

As mentioned above, CS are resistant to conventional chemotherapies. CS cell resistance can be explained in part by the structure of the tissue and its dense hyalin ECM composition, indicating that 3D models will become crucial tools to better understand the mechanism underlying CS drug resistance (Table 1). Comparison study between 2D and 3D chondrogenic spheroids from different origins (SW1353, CAL78 and OUMS27) and new established CS cell line from primary tumour biopsy (CH03, CH34

and CH56) showed that 3D CS spheroids were more resistant to chemotherapeutic drugs (Doxorubicin and Mafosfamide) than 2D cultures [127]. As shown by RT-qPCR, these cell lines cultured in 2D cells lost expression of several genes (*COL2A1*, *COMP*, *ACAN*) implicated in cartilage development that was restored in 3D cultures. Moreover, the capacity of each cell type to produce cartilaginous matrix was directly related to its drug resistance [127]. These data suggested a direct functional relationship between cartilaginous matrix composition and chemoresistance. Similarly, spheroids produced by CH2879, OUMS27 and L835 cell lines were used to determine the mechanism involved in resistance to cisplatin and doxorubicin [128]. 3D spheroids were generated by differentiation of cell lines after long period of culture (6 weeks in chondrogenic medium, see [129]) and exhibited CS phenotype. Exposure to chemotherapy agents highly activated the multidrug resistance pump (*ABCB1*) in all CS 3D spheroids. Inhibition of the anti-apoptotic *BCL-2* family members by specific drug (*ABT-737*) resulted in a sensitization of 3D CS to doxorubicin. These results indicated that tumour drug resistance does not rely only on ECM composition and that other mechanisms must be implied and be considered as potential targets for development of new CS therapies. Taken together, these data demonstrated that the mimicking of the cell behaviour and ECM of CS is the added value of 3D cultures. As discussed for OS, non-adherent surface methods can be used for obtaining multicellular tumour spheroids. Combination of non-adherent plates and 0.5% methylcellulose generated CS spheroids from the HEMC-SS cell line [130]. HEMC-SS spheroids developed CS tumour features as proliferative cell population at the periphery of a hypoxic and apoptotic core, with ECM rich in glycosaminoglycans and VEGF excretion (Fig. 4). Moreover, this model recapitulated the drug resistance phenotype observed in CS tumour for classical chemotherapy agents [130]. While still far for native tumour environment, the absence of complexity to generate this 3D system and its close features to the *in vivo* tumours make it a convincing model for massive drug screening. In this way, HEMC-SS spheroid model was used to evaluate the effect of new hypoxia-activated pro-drugs that target the rich proteoglycan ECM of CS [131]. This study showed that quaternary ammonium, which is characterised by a positive charge that interacts strongly with the negative charges present in the proteoglycans [132], could be used as an adjuvant for CS drug targeting [131]. Generation of CS 3D cultures by similar hanging-drop methods showed the potential of the ionophore salinomycin (*SAL*) as a new anti-CS drug [133]. *SAL* resulted in a strong cytotoxic effect in both 2D and 3D SW1353 (grade II) CS model by inducing cellular apoptosis via caspase activation [133]. Another approach to produce 3D CS system consists in the use of natural or synthetic material that can serve as substrates for the formation of tumour mass cells in cartilage or chondrosarcoma niches. Alginate hydrogels were used to analyse the invasion and drug resistance of CS models [134]. Compared to other biomaterials as collagen and Matrigel™, alginate is characterised by an inert and stable composition, which is translated in a more reproducible method to generate beads for encapsulation. Alginate encapsulated CH2879, JJ012 and SW1353 CS cell lines, compared to a 2D culture, were characterised by a long-term lifespan with generation of a hyaline-like cell matrix and demonstrated that 3D cultures recapitulated cell matrix gene expression. Interestingly, CH2879 cell line displayed an evasion phenotype from the beads compared to the other cell line models. This was somehow in coherence with the grade of malignancy III of this cell line whereas the other two are grade II. This data suggests that alginate beads are useful to analyse CS cell invasion properties. Thus, it can be combined with drug screening as alginate beads CS 3D model summed up the characteristic drug resistance phenotype of CS cell lines [134]. In agreement with this result and by using same methodology, Palubeckaite *et al.* showed that

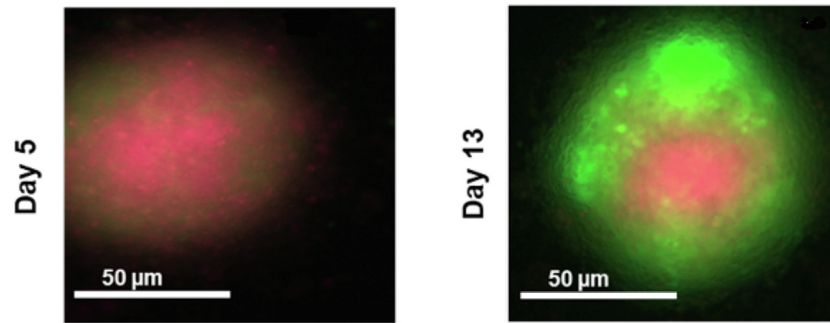


Fig. 4. Cell subpopulation in an OS spheroid. Spheroids are characterised by a continuum subset of cells that goes from apoptotic or bone-like MSC non-dividing cells (in red) to a peripheral proliferative subset of cells (green cells). 10,000 GFP-MNNG/HOS cells were seeded into a 96-multiwells low-attachment plate and cultured for 13 days. Pictures showed population evolution from day 5 to day 13. GFP expressing MNNG/HOS osteosarcoma cells stained with DiD (ThermoFisher) to show the retention of DiD by a non-proliferating subpopulation of the cells in the formed spheroid and imaged using fluorescent microscopy. Scale bar corresponds to 50 μm . (For interpretation of the references to colour in this figure legend, the reader is referred to the web version of this article.)

CS 3D spheroids reproduced similar phenotype that *in vivo* CS with production of an ECM enriched in collagen II and resistance to chemotherapeutic agents as doxorubicin, cisplatin, temozolomide and YM-155 [135].

CS are resistant to radiotherapy. Hamdi *et al.* developed a 3D approach to analyse the impact of linear energy transfer ionizing radiation (LET) in CS [136]. Due to its relative photon radioresistance, metastatic potential and cartilage phenotype, intermediate-grade II SW1353 CS cell line was used as a model. 3D culture was performed by using a collagen scaffold and hypoxic conditions (2% of O_2) to mimic *in vivo* cartilage environment. Exposition to low and high LET radiation showed that 3D cultures resulted in a more resistant phenotype with a delayed response of DNA repair mechanisms (evaluated by H2AX expression post radiation) than 2D cultures, where cell were grown in monolayer conditions and normoxia (20% oxygen). The main difference between culture methods relied in the microenvironment conditions, which implied that the microenvironment played a key role in the radiation resistance of CS and should be considered when determining the depth-dose profile in radiation therapy of SC [136].

2.3.1. Chondrosarcoma 3D culture approaches to investigate cell adhesion, migration and cell-to-cell interactions

3D CS cultures were used to determine the impact of TME charges during cell adhesion [137]. Titanium beads from 400 to 500 μm were modified by deposition of polyelectrolyte multilayer film that conferred a positive or negative surface charge. In the presence of negative charges, human HCS-2/8 CS cells exhibited cytoplasmic stress fibres that were totally absent when positive charged TME were tested, indicating that anionic charges affected cytoskeleton organisation. Moreover, anionic but not cationic surfaces promoted two modes of pseudopod formation by HCS-2/8 cells, in a random progression and as a “cell recognition signal”. This phenomenon was associated with a cellular mechanism to optimize the anchoring process. Interestingly, cells developed pseudopods on cationic surfaces when cells were cultured in the presence of conditioned medium obtained from an anionic culture, suggesting that this process was regulated by an exocytotic mechanism. This mechanism was linked to the MAPK ERK1/2 pathways as phosphorylation levels were increased in the presence of anionic charges and reduced when cationic surfaces were assessed [137]. Overall, these studies suggested that ECM has a relevant role in CS cell adhesion and migration.

As described for OS, direct or indirect cell–cell interactions between CS cells and cells of the local microenvironment can be analysed by combination of 3D and 2D cultures. In a recent study,

Minopoli *et al.* analysed the contribution of pro-tumoral M2 macrophages to CS development [138]. Primary CS cells were isolated from patient biopsies and cultured by hanging drop methods to produce 3D spheroids and then co-cultured in collagen/fibroblast matrix with blood isolated monocytes. The size of CS spheroids increased in the presence of monocytes, probably due to an increase of CS cell invasive capability induced by monocyte factors. And reciprocally, CS cells induced monocyte differentiation into a pro-tumoral M2 phenotype. These observations indicated a cross-talk between CS cells and macrophages through soluble mediators [138]. The induction of CS proliferation by macrophages was inhibited by the addition of urokinase receptor (uPAR)-derived synthetic peptide RI-3 which was known to reduce the monocyte migration [139]. In this context, RI-3 could potentially avoid the recruitment of monocytes to CS niches and reduce proliferation and angiogenic properties of CS tumour [138].

Recently, an innovative method was developed to assemble 3D CS spheroids by levitational forces by using low doses of gadobutrol salt [140]. As biological tissues are considered to be diamagnetic, they can be levitated when paramagnetic medium is used. Paramagnetic ions of Gadolinium(III) (Gd^{3+}) have been widely used as a contrast agent but are characterised by cytotoxicity at high concentrations and lower concentration of Gd^{3+} did not allow cell levitation. However, by using high magnetic fields, Parfeno *et al.* induced SW1353 CS spheroid magnetic levitational bio assembly in the presence of lower doses of gadobutrol (0.8 mM). The study revealed minimal cytotoxicity by the magnetic field and opens a new area in the domain of microgravity and tumour biology [140]. In the meantime, further studies may be needed to determine if high magnetic fields have an impact in cell behaviour, genomic and proteomic expression pattern.

3. Conclusion and future perspectives

Primary bone tumour progression and metastasis rely on the particular combination of bone MSC differentiation and physiological, structural, biochemical TME interactions. 2D cultures were considered for a long time as a valid approach for improving the knowledge in tumour biology. Many studies gave evidence that 2D cultures did not reflect the real nature of tumours, as many treatments that were effective in 2D failed in clinical trials. In this context, development of 3D culture approaches that mimic TME is a new perspective. In particular, the use of natural materials already presents in the bone ECM or synthetic materials as scaffolds for 3D bone culture generation demonstrates to be promising approaches for the study of tumour invasion, metastasis, angiogenesis processes and anti-tumour drug development. Moreover, the

development of novel technologies in 3D cultures as microfluidics and bioprinting that allow the generation of customizable 3D systems constitute a fully scientific revolution. These technologies can be combined with other 3D techniques and allow the creation of a fully controlled TME that reproduces the native configuration of bone tumours, including cell-to-cell or tissue interactions, cell adhesion, proliferation and migration, EMC structure and composition, physiology parameters as hypoxia, shear stress and mechanical forces. This 3D technological revolution will be an excellent opportunity for the identification of new bone therapeutic targets and drug discovery in bone sarcoma field.

Declaration of Competing Interest

The authors declare that they have no known competing financial interests or personal relationships that could have appeared to influence the work reported in this paper.

References

- [1] J.L. Ferguson, S.P. Turner, Bone cancer: diagnosis and treatment principles, *Am. Fam. Phys.* 98 (2018) 205–213, PMID: 30215968.
- [2] H.K. Brown, K. Schiavone, F. Gouin, M.F. Heymann, D. Heymann, Biology of bone sarcomas and new therapeutic developments, *Calcif Tissue Int.* 102 (2018) 174–195, <https://doi.org/10.1007/s00223-017-0372-2>.
- [3] D.D. Moore, H.H. Luu, Osteosarcoma, *Cancer Treat Res.* 162 (2014) 65–92, https://doi.org/10.1007/978-3-319-07323-1_4.
- [4] M. Kovac, C. Blattmann, S. Ribl, J. Smida, N.S. Mueller, F. Engert, F. Castro-Giner, J. Weischenfeldt, M. Kovacova, A. Krieg, D. Andreou, P.U. Tunn, H.R. Dürr, H. Rech, K.D. Schaser, I. Melcher, S. Burdach, A. Kulozik, K. Specht, K. Heinemann, S. Fulda, S. Bielack, G. Jundt, I. Tomlinson, J.O. Korbel, M. Nathrath, D. Baumhoer, Exome sequencing of osteosarcoma reveals mutation signatures reminiscent of BRCA deficiency, *Nat. Commun.* 6 (2015) 8940, <https://doi.org/10.1038/ncomms9940>.
- [5] H.K. Brown, M. Tellez-Gabriel, D. Heymann, Cancer stem cells in osteosarcoma, *Cancer Lett.* 386 (2017) 189–195, <https://doi.org/10.1016/j.canlet.2016.11.019>.
- [6] M.F. Heymann, F. Lézet, D. Heymann, The contribution of immune infiltrates and the local microenvironment in the pathogenesis of osteosarcoma, *Cell Immunol.* 343 (2019), <https://doi.org/10.1016/j.cellimm.2017.10.011>.
- [7] C. Yang, Y. Tian, F. Zhao, Z. Chen, P. Su, Y. Li, A. Qian, Bone microenvironment and osteosarcoma metastasis, *Int. J. Mol. Sci.* 21 (2020) 6985, <https://doi.org/10.3390/ijms21196985>.
- [8] J. Cui, D. Dean, F.J. Hornicek, Z. Chen, Z. Duan, The role of extracellular matrix in osteosarcoma progression and metastasis, *J. Exp. Clin. Cancer Res.* 39 (2020) 178, <https://doi.org/10.1186/s13046-020-01685-w>.
- [9] N.J. Balamuth, R.B. Womer, Ewing's sarcoma, *Lancet Oncol.* 11 (2010) 184–192, [https://doi.org/10.1016/S1470-2045\(09\)70286-4](https://doi.org/10.1016/S1470-2045(09)70286-4).
- [10] S. Renzi, N.D. Anderson, N. Light, A. Gupta, Ewing-like sarcoma: an emerging family of round cell sarcomas, *J. Cell Physiol.* 234 (2019) 7999–8007, <https://doi.org/10.1002/jcp.27558>.
- [11] F. Tirode, K. Laud-Duval, A. Prieur, B. Delorme, P. Charbord, O. Delattre, Mesenchymal stem cell features of Ewing tumors, *Cancer Cell.* 11 (2007) 421–429, <https://doi.org/10.1016/j.ccr.2007.02.027>.
- [12] R. Todorova, Ewing's sarcoma cancer stem cell targeted therapy, *Curr. Stem Cell Res. Ther.* 9 (2014) 46–62, <https://doi.org/10.2174/1574888x08666131203123125>.
- [13] S.E. Lamhamedi-Cherradi, M. Santoro, V. Ramammoorthy, B.A. Menegaz, G. Bartholomeusz, L.R. Iles, H.M. Amin, J.A. Livingston, A.G. Mikos, J.A. Ludwig, 3D tissue-engineered model of Ewing's sarcoma, *Adv. Drug Deliv. Rev.* 79–80 (2014) 155–171, <https://doi.org/10.1016/j.addr.2014.07.012>.
- [14] H. Yu, Y. Ge, L. Guo, L. Huang, Potential approaches to the treatment of Ewing's sarcoma, *Oncotarget* 8 (2017) 5523–5539, <https://doi.org/10.18632/oncotarget.12566>.
- [15] W.A. Chow, Chondrosarcoma: biology, genetics, and epigenetics, *F1000Res.* 7 (2018) 1826, <https://doi.org/10.12688/f1000research.15953.1>.
- [16] B. Mery, S. Espenel, J.B. Guy, C. Rancoule, A. Vallard, M.T. Aloy, C. Rodriguez-Lafresse, N. Magné, Biological aspects of chondrosarcoma: Leaps and hurdles, *Crit. Rev. Oncol. Hematol.* 123 (2018) 32–36, <https://doi.org/10.1016/j.critrevonc.2018.03.009>.
- [17] A.B. Shupp, A.D. Kolb, K.M. Bussard, Novel techniques to study the bone-tumor microenvironment, *Adv. Exp. Med. Biol.* 1225 (2020) 1–18, https://doi.org/10.1007/978-3-030-35727-6_1.
- [18] W. Roux, Beiträge zur Entwicklungsmechanik des Embryo, *Z. Biol.* 21 (1885) 411.
- [19] R.G. Harrison, The outgrowth of the nerve fiber as a mode of protoplasmic movement, *J. Exp. Zool.* 142 (1910) 5–73.
- [20] Z. Koledova, 3D cell culture: an introduction, *Methods Mol. Biol.* 1612 (2017) 1–11, https://doi.org/10.1007/978-1-4939-7021-6_1.
- [21] A.M. Sitarski, H. Fairfield, C. Falank, M.R. Reagan, 3d tissue engineered in vitro models of cancer in bone, *ACS Biomater. Sci. Eng.* 4 (2018) 324–336, <https://doi.org/10.1021/acsbomaterials.7b00097>.
- [22] H. Qiao, T. Tang, Engineering 3D approaches to model the dynamic microenvironments of cancer bone metastasis, *Bone Res.* 6 (2018) 3, <https://doi.org/10.1038/s41413-018-0008-9>.
- [23] N. Chaicharoenaudomrung, P. Kunhorn, P. Noisa, Three-dimensional cell culture systems as an in vitro platform for cancer and stem cell modeling, *World J. Stem Cells* 11 (2019) 1065–1083, <https://doi.org/10.4252/wjvsc.v11.i12.1065>.
- [24] A. De Luca, L. Raimondi, F. Salamanna, V. Carina, V. Costa, D. Bellavia, R. Alessandro, M. Fini, G. Giavaresi, Relevance of 3d culture systems to study osteosarcoma environment, *J. Exp. Clin. Cancer Res.* 37 (2018) 2, <https://doi.org/10.1186/s13046-017-0663-5>.
- [25] J.M. Kelm, N.E. Timmins, C.J. Brown, M. Fussenegger, L.K. Nielsen, Method for generation of homogeneous multicellular tumor spheroids applicable to a wide variety of cell types, *Biotechnol. Bioeng.* 83 (2) (2003) 173–180, [https://doi.org/10.1002/\(ISSN\)1097-029010.1002/bit.v83.2.10.1002/bit.10655](https://doi.org/10.1002/(ISSN)1097-029010.1002/bit.v83.2.10.1002/bit.10655).
- [26] R. Foty, A simple hanging drop cell culture protocol for generation of 3D spheroids, *J. Vis. Exp.* 51 (2011) 2720, <https://doi.org/10.3791/2720>.
- [27] S.W. Potter, J.E. Morris, Development of mouse embryos in hanging drop culture, *Anat. Rec.* 211 (1985) 48–56, <https://doi.org/10.1002/ar.1092110109>.
- [28] B.H. Reed, S.C. McMillan, R. Chaudhary, The preparation of Drosophila embryos for live-imaging using the hanging drop protocol, *J. Vis. Exp.* 25 (2009) 1206, <https://doi.org/10.3791/1206>.
- [29] K. Archacka, M. Pozzobon, A. Repele, C.A. Rossi, M. Campanella, P. De Coppi, Culturing muscle fibres in hanging drop: a novel approach to solve an old problem, *Mol. Cell* 106 (2014) 72–82, <https://doi.org/10.1111/boc.201300028>.
- [30] S. Wang, X. Wang, J. Boone, J. Wie, K.P. Yip, J. Zhang, L. Wang, R. Liu, Application of hanging drop technique for kidney tissue culture, *Kidney Blood Press Res.* 42 (2017) 220–231, <https://doi.org/10.1159/000476018>.
- [31] M. Panek, M. Grabacka, M. Pierzchalska, The formation of intestinal organoids in a hanging drop culture, *Cytotechnology* 70 (2018) 1085–1095, <https://doi.org/10.1007/s10616-018-0194-8>.
- [32] S.W. Huang, S.C. Tzeng, J.K. Chen, J.S. Sun, F.H. Lin, A dynamic hanging-drop system for mesenchymal stem cell culture, *Int. J. Mol. Sci.* 21 (2020) 4298, <https://doi.org/10.3390/ijms21124298>.
- [33] E. Carletti, A. Motta, C. Migliari, Scaffolds for tissue engineering and 3D cell culture, *Methods Mol. Biol.* 695 (2011) 17–39, https://doi.org/10.1007/978-1-60761-984-0_2.
- [34] A. Kamatar, G. Gunay, H. Acar, Natural and synthetic biomaterials for engineering multicellular tumor spheroids, *Polymers (Basel)* 12 (2020) 2506, <https://doi.org/10.3390/polym12112506>.
- [35] A.K. Kureshi, A. Afoko, S. Wohler, S. Barker, R.A. Brown, 3D culture model of fibroblast-mediated collagen creep to identify abnormal cell behaviour, *Biomech Model Mechanobiol.* 14 (2015) 1255–1263, <https://doi.org/10.1007/s10237-015-0672-2>.
- [36] A. Shahin-Shamsabadi, P.R. Selvaanapathy, A rapid biofabrication technique for self-assembled collagen-based multicellular and heterogeneous 3D tissue constructs, *Acta Biomater.* 92 (2019) 172–183, <https://doi.org/10.1016/j.actbio.2019.05.024>.
- [37] H.K. Kleinman, G.R. Martin, Matrigel: basement membrane matrix with biological activity, *Semin. Cancer Biol.* 15 (2005) 378–386, <https://doi.org/10.1016/j.semcancer.2005.05.004>.
- [38] S. Aoki, T. Takezawa, H. Sugihara, S. Toda, Progress in cell culture systems for pathological research, *Pathol. Int.* 66 (2016) 554–562, <https://doi.org/10.1111/pin.12443>.
- [39] T. Andersen, P. Auk-Emblem, M. Dornish, 3D cell culture in alginate hydrogels, *Microarrays (Basel)* 4 (2015) 33–61, <https://doi.org/10.3390/microarrays4020133>.
- [40] S. Fujita, Y. Wakuda, M. Matsumura, S.I. Suye, Geometrically customizable alginate hydrogel nanofibers for cell culture platforms, *J. Mater. Chem. B* 7 (2019) 6556–6563, <https://doi.org/10.1039/c9tb01353a>.
- [41] K. Xu, K. Ganapathy, T. Andl, Z. Wang, J.A. Copland, R. Chakrabarti, S.J. Florczyk, 3D porous chitosan-alginate scaffold stiffness promotes differential responses in prostate cancer cell lines, *Biomaterials* 217 (2019) 119311, <https://doi.org/10.1016/j.biomaterials.2019.119311>.
- [42] F. Gao, J. Li, L. Wang, D. Zhang, J. Zhang, F. Guan, M. Yao, Dual-enzymatically crosslinked hyaluronic acid hydrogel as a long-time 3D stem cell culture system, *Biomed. Mater.* 15 (2020) 045013, <https://doi.org/10.1088/1748-605X/ab712e>.
- [43] P. Maleki Dana, J. Hallajzadeh, Z. Asemi, M.A. Mansournia, B. Yousefi, Chitosan applications in studying and managing osteosarcoma, *Int. J. Biol. Macromol.* 169 (2021) 321–329, <https://doi.org/10.1016/j.ijbiomac.2020.12.058>.
- [44] E.A. Aisenbrey, W.L. Murphy, Synthetic alternatives to Matrigel, *Nat. Rev. Mater.* 5 (2020) 539–551, <https://doi.org/10.1038/s41578-020-0199-8>.
- [45] M.H. Park, H.J. Moon, J.H. Park, U.P. Shinde, Y. Ko du, B. Jeong, PEG-Poly(L-alanine) thermogel as a 3D scaffold of bone-marrow-derived mesenchymal stem cells, *Macromol. Biosci.* 15 (2015) 464–472, <https://doi.org/10.1002/mabi.201400426>.
- [46] H. Song, G. Yang, P. Huang, D. Kong, W. Wang, Self-assembled PEG-poly(L-valine) hydrogels as promising 3D cell culture scaffolds, *J. Mater. Chem. B* 5 (2017) 1724–1733, <https://doi.org/10.1039/c6tb02969h>.
- [47] S. Pradhan, I. Hassani, W.J. Seeto, E.A. Lipke, PEG-fibrinogen hydrogels for three-dimensional breast cancer cell culture, *J. Biomed. Mater. Res. A* 105 (2017) 236–252, <https://doi.org/10.1002/jbm.a.35899>.

- [48] Y. Wang, X. Cao, M. Ma, W. Lu, B. Zhang, Y. Guo, A GelMA-PEGDA-nHA composite hydrogel for bone tissue engineering, *Materials (Basel)* 13 (2020) 3735, <https://doi.org/10.3390/ma13173735>.
- [49] S.N. Bhatia, D.E. Ingber, Microfluidic organs-on-chips, *Nat. Biotechnol.* 32 (2014) 760–772, <https://doi.org/10.1038/nbt.2989>.
- [50] M. Mehling, S. Tay, Microfluidic cell culture, *Curr. Opin. Biotechnol.* 25 (2014) 95–102, <https://doi.org/10.1016/j.copbio.2013.10.005>.
- [51] B. Byambaa, N. Annabi, K. Yue, G. Trujillo-de Santiago, M.M. Alvarez, W. Jia, M. Kazemzadeh-Narbat, S.R. Shin, A. Tamayol, A. Khademhosseini, Bioprinted osteogenic and vasculogenic patterns for engineering 3D bone tissue, *Adv. Healthc. Mater.* 6 (2017), <https://doi.org/10.1002/adhm.201700015>.
- [52] R. Mittal, F.W. Woo, C.S. Castro, M.A. Cohen, J. Karanxha, J. Mittal, T. Chhibber, V.M. Jhaveri, Organ-on-chip models: implications in drug discovery and clinical applications, *J. Cell Physiol.* 234 (2019) 8352–8380, <https://doi.org/10.1002/jcp.27729>.
- [53] A.D. Suarez-Martinez, M. Sole-Gras, S.S. Dykes, Z.R. Wakefield, K. Bauer, D. Majbour, A. Bundy, C. Pampo, M.E. Burrow, D.W. Siemann, Y. Huang, W.L. Murfee, Bioprinting on live tissue for investigating cancer cell dynamics, *Tissue Eng. Part A* (2020), <https://doi.org/10.1089/ten.TEA.2020.0190>, Online ahead of print.
- [54] M.D. Brennan, M.L. Rexius-Hall, L.J. Elgass, D.T. Eddington, Oxygen control with microfluidics, *Lab Chip* 14 (2014) 4305–4318, <https://doi.org/10.1039/c4lc00853g>.
- [55] J. Ahn, J. Lim, N. Jusoh, J. Lee, T.E. Park, Y. Kim, J. Kim, N.L. Jeon, 3D microfluidic bone tumor microenvironment comprised of hydroxyapatite/fibrin composite, *Front Bioeng Biotechnol.* 7 (2019) 168, <https://doi.org/10.3389/fbioe.2019.00168>.
- [56] I. Desyatnik, M. Krasner, L. Frolov, M. Ronen, O. Guy, D. Wasserman, A. Tzur, D. Avrahami, E. Barbiro-Michaely, D. Gerber, An integrated microfluidics approach for personalized cancer drug sensitivity and resistance assay, *Adv. Biosyst.* 3 (2019) e1900001, <https://doi.org/10.1002/adbi.201900001>.
- [57] S. Bersini, J.S. Jeon, G. Dubini, C. Arrigoni, S. Chung, J.L. Charest, M. Moretti, R. D. Kamm, A microfluidic 3D in vitro model for specificity of breast cancer metastasis to bone, *Biomaterials* 35 (2014) 2454–2461, <https://doi.org/10.1016/j.biomaterials.2013.11.050>.
- [58] T. Almela, S. Al-Sahaf, I.M. Brook, K. Khoshroo, M. Rasoulianboroujeni, F. Fahimipour, M. Tahrii, E. Dashtimoghdam, R. Bolt, L. Tayebi, K. Moharamzadeh, 3D printed tissue engineered model for bone invasion of oral cancer, *Tissue Cell* 52 (2018) 71–77, <https://doi.org/10.1016/j.tice.2018.03.009>.
- [59] N.M. Wragg, D. Mosqueira, L. Blokpeol-Ferreras, A. Capel, D.J. Player, N.R.W. Martin, Y. Liu, M.P. Lewis, Development of a 3D tissue-engineered skeletal muscle and bone co-culture system, *Biotechnol. J.* 15 (2020) e1900106, <https://doi.org/10.1002/biot.201900106>.
- [60] X. Liu, H. Lin, J. Song, T. Zhang, X. Wang, X. Huang, C. Zheng, A Novel SimpleDrop Chip for 3D Spheroid Formation and Anti-Cancer Drug Assay, *Micromachines (Basel)* 12 (6) (2021) 681, <https://doi.org/10.3390/mi12060681>.
- [61] M. Rimann, S. Laternser, A. Gvozdenovic, R. Muff, B. Fuchs, J.M. Kelm, U. Graf-Hausner, An in vitro osteosarcoma 3D microtissue model for drug development, *J. Biotechnol.* 189 (2014) 129–135, <https://doi.org/10.1016/j.jbiotec.2014.09.005>.
- [62] N. Baek, O.W. Seo, M. Kim, J. Hulme, S.S. An, Monitoring the effects of doxorubicin on 3D-spheroid tumor cells in real-time, *Oncol. Targets Ther.* 9 (2016) 7207–7218, <https://doi.org/10.2147/OTT.S112566>.
- [63] I.E. León, J.F. Cadavid-Vargas, A. Resasco, F. Maschi, M.A. Ayala, C. Carbone, S. B. Etcheverry, In vitro and in vivo antitumor effects of the VO-chrysin complex on a new three-dimensional osteosarcoma spheroids model and a xenograft tumor in mice, *J. Biol. Inorg. Chem.* 21 (2016) 1009–1020, <https://doi.org/10.1007/s00775-016-1397-0>.
- [64] P. Thanindrataran, X. Li, D.C. Dean, S.D. Nelson, F.J. Hornicek, Z. Duan, Establishment and characterization of a recurrent osteosarcoma cell line: OSA 1777, *J. Orthop. Res.* 38 (2020) 902–910, <https://doi.org/10.1002/jor.24528>.
- [65] S. Lenna, C. Bellotti, S. Duchi, E. Martella, M. Columbaro, B. Dozza, M. Ballestri, A. Guerrini, G. Sorgiu, T. Frisoni, L. Cevolani, G. Varchi, M. Ferrari, D.M. Donati, E. Lucarelli, Mesenchymal stromal cells mediated delivery of photoactive nanoparticles inhibits osteosarcoma growth in vitro and in a murine in vivo ectopic model, *J. Exp. Clin. Cancer Res.* 39 (2020) 40, <https://doi.org/10.1186/s13046-020-01548-4>.
- [66] A. Kiss, A.P. Ráduly, Z. Regdon, Z. Polgár, S. Tarapcsák, I. Sturniolo, T. El-Hamoly, L. Virág, C. Hegedűs, Targeting Nuclear NAD⁺ Synthase Inhibits DNA Repair, impairs metabolic adaptation and increases chemosensitivity of U-2OS osteosarcoma cells, *Cancers (Basel)* 12 (2020) 1180, <https://doi.org/10.3390/cancers12051180>.
- [67] P.A. Netti, D.A. Berk, M.A. Swartz, A.J. Grodzinsky, R.K. Jain, Role of extracellular matrix assembly in interstitial transport in solid tumors, *Cancer Res.* 60 (2000) 2497–2503.
- [68] K. Akeda, A. Nishimura, H. Satonaka, K. Shintani, K. Kusuzaki, A. Matsumine, Y. Kasai, K. Masuda, A. Uchida, Three-dimensional alginate spheroid culture system of murine osteosarcoma, *Oncol. Rep.* 22 (2009) 997–1003, <https://doi.org/10.3892/or.00000527>.
- [69] P.H. Tan, S.S. Chia, S.L. Toh, J.C. Goh, S.S. Nathan, Three-dimensional spatial configuration of tumour cells confers resistance to chemotherapy independent of drug delivery, *J. Tissue Eng. Regen. Med.* 10 (2016) 637–646, <https://doi.org/10.1002/term.1800>.
- [70] D.C. Belisario, M. Akman, M. Godel, V. Campani, M.P. Patrizio, L. Scotti, C.M. Hattinger, G. De Rosa, M. Donadelli, M. Serra, J. Kopecka, C. Riganti, ABCA1/ABCB1 ratio determines chemo- and immune-sensitivity in human osteosarcoma, *Cells* 9 (2020) 647, <https://doi.org/10.3390/cells9030647>.
- [71] T. Jiang, J. Zhao, S. Yu, Z. Mao, C. Gao, Y. Zhu, C. Mao, L. Zheng, Untangling the response of bone tumor cells and bone forming cells to matrix stiffness and adhesion ligand density by means of hydrogels, *Biomaterials* 188 (2019) 130–143, <https://doi.org/10.1016/j.biomaterials.2018.10.015>, Erratum in: *Biomaterials*. 231(2020) 119663.
- [72] T. Jiang, G. Xu, X. Chen, X. Huang, J. Zhao, L. Zheng, Impact of Hydrogel Elasticity and Adherence on Osteosarcoma Cells and Osteoblasts, *Adv Healthc Mater.* 8 (2019) e1801587, <https://doi.org/10.1002/adhm.201801587>, Erratum in: *Adv Healthc Mater.* (9) 2020 e2000054.
- [73] E.R. Molina, L.K. Chim, M.C. Salazar, S.M. Mehta, B.A. Menegaz, S.E. Lamhamedi-Cherradi, T. Satish, S. Mohiuddin, D. McCall, A.M. Zaske, B. Cuglievan, A.J. Lazar, D.W. Scott, J.K. Grande-Allen, J.A. Ludwig, A.G. Mikos, Mechanically tunable coaxial electrospun models of YAP/TAZ mechanoresponse and IGF-1R activation in osteosarcoma, *Acta Biomater.* 100 (2019) 38–51, <https://doi.org/10.1016/j.actbio.2019.09.029>.
- [74] B. Fallica, J.S. Maffei, S. Villa, G. Makin, M. Zaman, Alteration of cellular behavior and response to PI3K pathway inhibition by culture in 3D collagen gels, *PLoS One* 7 (2012) e48024, <https://doi.org/10.1371/journal.pone.0048024>.
- [75] S. Marastoni, G. Ligresti, E. Lorenzon, A. Colombatti, M. Mongiat, Extracellular matrix: a matter of life and death, *Connect Tissue Res.* 49 (2008) 203–206, <https://doi.org/10.1080/03080200802143190>.
- [76] K.M. Charoen, B. Fallica, Y.L. Colson, M.H. Zaman, M.W. Grinstaff, Embedded multicellular spheroids as a biomimetic 3D cancer model for evaluating drug and drug-device combinations, *Biomaterials* 35 (2014) 2264–2271, <https://doi.org/10.1016/j.biomaterials.2013.11.038>.
- [77] C. Bai, M. Yang, Z. Fan, S. Li, T. Gao, Z. Fang, Associations of chemo- and radio-resistant phenotypes with the gap junction, adhesion and extracellular matrix in a three-dimensional culture model of soft sarcoma, *J. Exp. Clin. Cancer Res.* 34 (2015) 58, <https://doi.org/10.1186/s13046-015-0175-0>.
- [78] I. Palubeckaitė, L. Crooks, D.P. Smith, L.M. Cole, H. Bram, C. Le Maitre, M.R. Clench, N.A. Cross, Mass spectrometry imaging of endogenous metabolites in response to doxorubicin in a novel 3D osteosarcoma cell culture model, *J. Mass Spectrom.* 55 (2020) e4461, <https://doi.org/10.1002/jms.4461>.
- [79] D.W. Green, E.J. Kim, H.S. Jung, Spontaneous gene transfection of human bone cells using 3D mineralized alginate-chitosan microcapsules, *J. Biomed. Mater. Res. A* 103 (2015) 2855–2863, <https://doi.org/10.1002/jbm.a.35414>.
- [80] C. Gorgun, S. Ozturk, S. Gokalp, S. Vatanever, S.I. Gurhan, A.S. Urkmez, Synergistic role of three dimensional niche and syx10a on conservation of cancer stem cell phenotype, *Int. J. Biol. Macromol.* 90 (2016) 20–26, <https://doi.org/10.1016/j.ijbiomac.2015.12.053>.
- [81] L. Barbato, M. Bocchetti, A. Di Biase, T. Regad, Cancer stem cells and targeting strategies, *Cells* 8 (2019) 926, <https://doi.org/10.3390/cells8080926>.
- [82] F.M. Vallette, C. Olivier, F. Lézot, L. Oliver, D. Cochinneau, L. Laliér, P.F. Cartron, D. Heymann, Dormant, quiescent, tolerant and persister cells: Four synonyms for the same target in cancer, *Biochem. Pharmacol.* 162 (2019) 169–176, <https://doi.org/10.1016/j.bcp.2018.11.004>.
- [83] S. Ozturk, C. Gorgun, S. Gokalp, S. Vatanever, A. Sendemir, Development and characterization of cancer stem cell-based tumoroids as an osteosarcoma model, *Biotechnol. Bioeng.* 117 (2020) 2527–2539, <https://doi.org/10.1002/bit.27381>.
- [84] G. Bassi, S. Panseri, S.M. Dozio, M. Sandri, E. Campodoni, M. Dapporto, S. Sprio, A. Tampieri, M. Montesi, Scaffold-based 3D cellular models mimicking the heterogeneity of osteosarcoma stem cell niche, *Sci. Rep.* 10 (2020) 22294, <https://doi.org/10.1038/s41598-020-79448-y>.
- [85] J. Tornín, A. Villasante, X. Solé-Martí, M.P. Ginebra, C. Canal, Osteosarcoma tissue-engineered model challenges oxidative stress therapy revealing promoted cancer stem cell properties, *Free Radic. Biol. Med.* 164 (2021) 107–118, <https://doi.org/10.1016/j.freeradbiomed.2020.12.437>.
- [86] C. Gebhard, I. Müller, K. Hummel, M. Neschi Née Ondrovics, S. Schlosser, I. Walter, Comparative proteomic analysis of monolayer and spheroid culture of canine osteosarcoma cells, *J. Proteomics* 177 (2018) 124–136, <https://doi.org/10.1016/j.jprotp.2018.01.006>.
- [87] C. Trojani, P. Weiss, J.F. Michiels, C. Vinatier, J. Guicheux, G. Daculsi, P. Gaudray, G.F. Carle, N. Rochet, Three-dimensional culture and differentiation of human osteogenic cells in an injectable hydroxypropylmethylcellulose hydrogel, *Biomaterials* 26 (2005) 5509–5517, <https://doi.org/10.1016/j.biomaterials.2005.02.001>.
- [88] G. Turnbull, J. Clarke, F. Picard, P. Riches, L. Jia, F. Han, B. Li, W. Shu, 3D bioactive composite scaffolds for bone tissue engineering, *Bioact Mater.* 3 (2017) 278–314, <https://doi.org/10.1016/j.bioactmat.2017.10.001>.
- [89] X. Liu, A.E. Jakus, M. Kural, H. Qian, A. Engler, M. Ghaedi, R. Shah, D.M. Steinbacher, L.E. Niklason, Vascularization of Natural and Synthetic Bone Scaffolds, *Cell Transplant* 27 (2018) 1269–1280, <https://doi.org/10.1177/0963689718782452>.
- [90] G. Picone, C. Cappadone, A. Pasini, J. Lovecchio, M. Cortesi, G. Farruggia, M. Lombardo, A. Gianoncelli, L. Mancini, H.M. Ralf, S. Donato, E. Giordano, E. Malucelli, S. Iotti, Analysis of Intracellular Magnesium and Mineral Depositions during Osteogenic Commitment of 3D Cultured Saos2 Cells, *Int. J. Mol. Sci.* 21 (2020) 2368, <https://doi.org/10.3390/ijms21072368>.
- [91] M. Prideaux, A.R. Wijenayaka, D.D. Kumarasinghe, R.T. Ormsby, A. Evdokiou, D.M. Findlay, G.J. Atkins, SaOS2 Osteosarcoma cells as an in vitro model for

- studying the transition of human osteoblasts to osteocytes, *Calcif Tissue Int.* 95 (2014) 183–193, <https://doi.org/10.1007/s00223-014-9879-y>.
- [92] T. Kihara, C. Umezumi, K. Sawada, Y. Furutani, Osteogenic cells form mineralized particles, a few μm in size, in a 3D collagen gel culture, *PeerJ* 7 (2019) e7889, <https://doi.org/10.7717/peerj.7889>.
- [93] D. Couchourel, C. Escoffier, R. Rohanizadeh, S. Bohic, G. Daculsi, Y. Fortun, M. Padrines, Effects of fibronectin on hydroxyapatite formation, *J. Inorg. Biochem.* 73 (1999) 129–136, [https://doi.org/10.1016/S0162-0134\(99\)00006-9](https://doi.org/10.1016/S0162-0134(99)00006-9).
- [94] M. Padrines, R. Rohanizadeh, C. Damiens, D. Heymann, Y. Fortun, Inhibition of apatite formation by vitronectin, *Connect Tissue Res.* 41 (2000) 101–108, <https://doi.org/10.3109/03008200009067662>.
- [95] R. Rohanizadeh, M. Padrines, J.M. Boulter, D. Couchourel, Y. Fortun, G. Daculsi, Apatite precipitation after incubation of biphasic calcium-phosphate ceramic in various solutions: influence of seed species and proteins, *J. Biomed. Mater. Res.* 42 (1998) 530–539, [https://doi.org/10.1002/\(sici\)1097-4636\(19981215\)42:4<530::aid-jbm8>3.0.co;2-6](https://doi.org/10.1002/(sici)1097-4636(19981215)42:4<530::aid-jbm8>3.0.co;2-6).
- [96] J.P. Vanderburgh, S.A. Guelcher, J.A. Sterling, 3D bone models to study the complex physical and cellular interactions between tumor and the bone microenvironment, *J. Cell Biochem.* 119 (2018) 5053–5059, <https://doi.org/10.1002/jcb.26774>.
- [97] M. Stoppato, E. Carletti, D. Maniglio, C. Migliaresi, A. Motta, Functional role of scaffold geometries as a template for physiological ECM formation: evaluation of collagen 3D assembly, *J. Tissue Eng. Regen. Med.* 7 (2013) 161–168, <https://doi.org/10.1002/term.516>.
- [98] R. Riesco, L. Boyer, S. Blasse, P.M. Lefebvre, P. Assemet, T. Leichle, A. Accardo, L. Malaquin, Water-in-PDMS emulsion templating of highly interconnected porous architectures for 3D cell culture, *ACS Appl. Mater. Interfaces* 11 (2019) 28631–28640, <https://doi.org/10.1021/acsami.9b07564>.
- [99] S. Sarkar, C.C. Peng, Y.C. Tung, Comparison of VEGF-A secretion from tumor cells under cellular stresses in conventional monolayer culture and microfluidic three-dimensional spheroid models, *PLoS One* 15 (2020) e0240833, <https://doi.org/10.1371/journal.pone.0240833>.
- [100] M. Gorska, P.B. Krzywiec, A. Kuban-Jankowska, M. Zmijewski, M. Wozniak, J. Wierzbicka, A. Piotrowska, K. Siwicka, Growth inhibition of osteosarcoma cell lines in 3D cultures: role of nitrosative and oxidative stress, *Anticancer Res.* 36 (2016) 221–229.
- [101] A.L. Gamblin, A. Renaud, C. Charrier, P. Hulin, G. Louarn, D. Heymann, V. Trichet, P. Layrolle, Osteoblastic and osteoclastic differentiation of human mesenchymal stem cells and monocytes in a miniaturized three-dimensional culture with mineral granules, *Acta Biomater.* 10 (2014) 5139–5147, <https://doi.org/10.1016/j.actbio.2014.08.033>.
- [102] H.T. Sasmazel, Novel hybrid scaffolds for the cultivation of osteoblast cells, *Int. J. Biol. Macromol.* 49 (2011) 838–846, <https://doi.org/10.1016/j.ijbiomac.2011.07.022>.
- [103] K. Zafeiris, D. Brasinika, A. Karatza, E. Koumoulos, I.K. Karoussis, K. Kyriakidou, C.A. Charitidis, Additive manufacturing of hydroxyapatite-chitosan-genipin composite scaffolds for bone tissue engineering applications, *Mater. Sci. Eng. C Mater. Biol. Appl.* 119 (2021) 111639, <https://doi.org/10.1016/j.msec.2020.111639>.
- [104] C. Chen, K. Chen, S.T. Yang, Effects of three-dimensional culturing on osteosarcoma cells grown in a fibrous matrix: analyses of cell morphology, cell cycle, and apoptosis, *Biotechnol. Prog.* 19 (2003) 1574–1582, <https://doi.org/10.1021/bp034024w>.
- [105] V.L. Thai, K.H. Griffin, S.W. Thorpe, R.L. Randall, J.K. Leach, Tissue engineered platforms for studying primary and metastatic neoplasm behavior in bone, *J. Biomech.* 115 (2021) 110189, <https://doi.org/10.1016/j.jbiomech.2020.110189>.
- [106] S. Hao, L. Ha, G. Cheng, Y. Wan, Y. Xia, D.M. Sosnoski, A.M. Mastro, S.Y. Zheng, A spontaneous 3D bone-on-a-chip for bone metastasis study of breast cancer cells, *Small* 14 (2018) e1702787, <https://doi.org/10.1002/smll.201702787>.
- [107] S. Choudhary, P. Ramasundaram, E. Dziopa, C. Mannion, Y. Kissin, L. Tricoli, C. Albanese, W. Lee, J. Zilberberg, Human ex vivo 3D bone model recapitulates osteocyte response to metastatic prostate cancer, *Sci. Rep.* 8 (2018) 17975, <https://doi.org/10.1038/s41598-018-36424-x>.
- [108] P.S. Raman, C.D. Paul, K.M. Stroka, K. Konstantopoulos, Probing cell traction forces in confined microenvironments, *Lab Chip* 13 (2013) 4599–4607, <https://doi.org/10.1039/c3lc50802a>.
- [109] H. Chaddad, S. Kuchler-Bopp, G. Fuhrmann, H. Gegout, G. Ubeaud-Sequier, P. Schwinté, F. Bornert, N. Benkirane-Jessel, Y. Idoux-Gillet, Combining 2D angiogenesis and 3D osteosarcoma microtissues to improve vascularization, *Exp. Cell Res.* 360 (2017) 138–145, <https://doi.org/10.1016/j.yexcr.2017.08.035>.
- [110] M. Massimini, R. De Maria, D. Malatesta, M. Romanucci, A. D'Anselmo, Salda L. Della, Establishment of three-dimensional canine osteosarcoma cell lines showing vasculogenic mimicry and evaluation of biological properties after treatment with 17-AAG, *Vet. Comp. Oncol.* 17 (2019) 376–384, <https://doi.org/10.1111/vco.12482>.
- [111] E.L. Fong, S.E. Lamhamedi-Cherradi, E. Burdett, V. Ramamoorthy, A.J. Lazar, F. K. Kasper, M.C. Farach-Carson, D. Vishwamitra, E.G. Demicco, B.A. Menegaz, H.M. Amin, A.G. Mikos, J.A. Ludwig, Modeling Ewing sarcoma tumors in vitro with 3D scaffolds, *Proc. Natl. Acad. Sci. U.S.A.* 110 (2013) 6500–6505, <https://doi.org/10.1073/pnas.1221403110>.
- [112] K.A. Boehme, J. Nitsch, R. Riester, R. Handgretinger, S.B. Schleicher, T. Kluba, F. Traub, Arsenic trioxide potentiates the effectiveness of epiderisin in Ewing sarcomas, *Int. J. Oncol.* 49 (2016) 2135–2146, <https://doi.org/10.3892/ijo.2016.3700>.
- [113] M. Santoro, S.E. Lamhamedi-Cherradi, B.A. Menegaz, J.A. Ludwig, A.G. Mikos, Flow perfusion effects on three-dimensional culture and drug sensitivity of Ewing sarcoma, *Proc. Natl. Acad. Sci. U.S.A.* 112 (2015) 10304–10309, <https://doi.org/10.1073/pnas.1506684112>.
- [114] E.R. Molina, L.K. Chim, M.C. Salazar, G.L. Koons, B.A. Menegaz, A. Ruiz-Velasco, S.E. Lamhamedi-Cherradi, A.M. Vetter, T. Satish, B. Cuglievan, M.M. Smoak, D. W. Scott, J.A. Ludwig, A.G. Mikos, 3D Tissue-Engineered Tumor Model for Ewing's sarcoma that incorporates bone-like ECM and mineralization., *ACS Biomater. Sci. Eng.* 6 (2020) 539–552, <https://doi.org/10.1021/acsbomaterials.9b01068>.
- [115] A. Marturano-Kruik, A. Villasante, K. Yaeger, S.R. Ambati, A. Chramiec, M.T. Raimondi, G. Vunjak-Novakovic, Biomechanical regulation of drug sensitivity in an engineered model of human tumor, *Biomaterials* 150 (2018) 150–161, <https://doi.org/10.1016/j.biomaterials.2017.10.020>.
- [116] W.A. May, R.S. Grigoryan, N. Keshelava, D.J. Cabral, L.L. Christensen, J. Jenabi, L. Ji, T.J. Triche, E.R. Lawlor, K.P. Reynolds, Characterization and drug resistance patterns of Ewing's sarcoma family tumor cell lines, *PLoS One* 8 (2013) e80060, <https://doi.org/10.1371/journal.pone.0080060>.
- [117] K. Leuchte, B. Altvater, S. Hoffschlag, J. Potratz, J. Meltzer, D. Clemens, A. Luecke, J. Hards, U. Dirksen, H. Juergens, S. Kailayangiri, C. Rossig, Anchorage-independent growth of Ewing sarcoma cells under serum-free conditions is not associated with stem-cell like phenotype and function, *Oncol. Rep.* 32 (2014) 845–852, <https://doi.org/10.3892/or.2014.3269>.
- [118] A. Villasante, A. Marturano-Kruik, G. Vunjak-Novakovic, Bioengineered human tumor within a bone niche, *Biomaterials* 35 (2014) 5785–5794, <https://doi.org/10.1016/j.biomaterials.2014.03.081>.
- [119] A. Marturano-Kruik, A. Villasante, G. Vunjak-Novakovic, Bioengineered Models of Solid Human Tumors for Cancer Research, *Methods Mol Biol.* 1502 (2016) 203–11, https://doi.org/10.1007/978-1-4939-9353-3_11. Erratum in: *Methods Mol Biol.* 1502 (2016) E1.
- [120] S. Riffle, R.N. Pandey, M. Albert, R.S. Hegde, Linking hypoxia, DNA damage and proliferation in multicellular tumor spheroids, *BMC Cancer* 17 (2017) 338, <https://doi.org/10.1186/s12885-017-3319-0>.
- [121] G. Domenici, R. Eduardo, H. Castillo-Ecija, G. Orive, Á. Montero Carcaboso, C. Brito, PDX-Derived Ewing's sarcoma cells retain high viability and disease phenotype in alginate encapsulated spheroid cultures, *Cancers (Basel)* 13 (2021) 879, <https://doi.org/10.3390/cancers13040879>.
- [122] S. Riffle, R.S. Hegde, Modeling tumor cell adaptations to hypoxia in multicellular tumor spheroids, *J. Exp. Clin. Cancer Res.* 36 (2017) 102, <https://doi.org/10.1186/s13046-017-0570-9>.
- [123] E. David, F. Blanchard, M.F. Heymann, G. De Pinieux, F. Gouin, F. Rédini, D. Heymann, The bone niche of chondrosarcoma: a sanctuary for drug resistance, tumour growth and also a source of new therapeutic targets, *Sarcoma* 2011 (2011) 932451, <https://doi.org/10.1155/2011/932451>.
- [124] H.L. Evans, A.G. Ayala, M.M. Romsdahl, Prognostic factors in chondrosarcoma of bone: a clinicopathologic analysis with emphasis on histologic grading, *Cancer* 40 (1977) 818–831, [https://doi.org/10.1002/1097-0142\(197708\)40:2<818::aid-cnrc2820400234>3.0.co;2-b](https://doi.org/10.1002/1097-0142(197708)40:2<818::aid-cnrc2820400234>3.0.co;2-b).
- [125] S. Boeuf, E. Steck, K. Pelttari, T. Hennig, A. Buneb, K. Benz, D. Witte, H. Sültmann, A. Poustka, W. Richter, Subtractive gene expression profiling of articular cartilage and mesenchymal stem cells: serpins as cartilage-relevant differentiation markers, *Osteoarthritis Cartilage* 16 (2008) 48–60, <https://doi.org/10.1016/j.joca.2007.05.008>.
- [126] S. Boeuf, P. Kunz, T. Hennig, B. Lehner, P. Hogendoorn, J. Bovée, W. Richter, A chondrogenic gene expression signature in mesenchymal stem cells is a classifier of conventional central chondrosarcoma, *J. Pathol.* 216 (2008) 158–166, <https://doi.org/10.1002/path.2389>.
- [127] D. Monderer, A. Luseau, A. Bellec, E. David, S. Ponsolle, S. Saiagh, S. Bercegeay, P. Piloquet, M.G. Denis, L. Lodé, F. Rédini, M. Biger, D. Heymann, M.F. Heymann, R. Le Bot, F. Gouin, F. Blanchard, New chondrosarcoma cell lines and mouse models to study the link between chondrogenesis and chemoresistance, *Lab Invest.* 93 (2013) 1100–1114, <https://doi.org/10.1038/labinvest.2013.101>.
- [128] J.G. Van Oosterwijk, B. Herpers, D. Meijer, I.H. Briaire-de Bruijn, A.M. Cleton-Jansen, H. Gelderblom, B. van de Water, J.V. Bovée, Restoration of chemosensitivity for doxorubicin and cisplatin in chondrosarcoma in vitro: BCL-2 family members cause chemoresistance, *Ann. Oncol.* 23 (2012) 1617–1626, <https://doi.org/10.1093/annonc/mdr512>.
- [129] C.M. Reijnders, C.J. Waaijer, A. Hamilton, E.P. Buddingh, S.P. Dijkstra, J. Ham, E. Bakker, K. Szuhai, M. Karperien, P.C. Hogendoorn, S.E. Stringer, J.V. Bovée, No haploinsufficiency but loss of heterozygosity for EXT in multiple osteochondromas, *Am. J. Pathol.* 177 (2010) 1946–1957, <https://doi.org/10.2353/ajpath.2010.100296>.
- [130] A. Voissiere, E. Jouberton, E. Maubert, F. Degoul, C. Peyrode, J.M. Chezal, É. Miot-Noirault, Development and characterization of a human three-dimensional chondrosarcoma culture for in vitro drug testing, *PLoS One* 12 (2017) e0181340, <https://doi.org/10.1371/journal.pone.0181340>.
- [131] A. Voissiere, V. Weber, Y. Gerard, F. Rédini, F. Raes, J.M. Chezal, F. Degoul, C. Peyrode, E. Miot-Noirault, Proteoglycan-targeting applied to hypoxia-activated prodrug therapy in chondrosarcoma: first proof-of-concept, *Oncotarget* 8 (2017) 95824–95840, <https://doi.org/10.18632/oncotarget.21337>.
- [132] C. Peyrode, V. Weber, E. David, A. Vidal, P. Auzeloux, Y. Communal, M.M. Dauplat, S. Besse, F. Gouin, D. Heymann, J.M. Chezal, F. Rédini, E. Miot-Noirault, Quaternary ammonium-melphalan conjugate for anticancer therapy of chondrosarcoma: in vitro and in vivo preclinical studies, *Invest. New Drugs* 30 (2012) 1782–1790, <https://doi.org/10.1007/s10637-011-9663-z>.

- [133] F. Perut, F.V. Sbrana, S. Avnet, A. De Milito, N. Baldini, Spheroid-based 3D cell cultures identify salinomycin as a promising drug for the treatment of chondrosarcoma, *J. Orthop. Res.* (2018), <https://doi.org/10.1002/jor.23880>, Online ahead of print.
- [134] E. Lhuissier, C. Bazille, J. Aury-Landas, N. Girard, J. Pontin, M. Boittin, K. Boumediene, C. Baugé, Identification of an easy to use 3D culture model to investigate invasion and anticancer drug response in chondrosarcomas, *BMC Cancer* 17 (2017) 490, <https://doi.org/10.1186/s12885-017-3478-z>.
- [135] I. Palubeckaitė, S. Venneker, I.H. Briaire-de Bruijn, B.E. van den Akker, A.D. Krol, H. Gelderblom, J.V.M.G. Bovée, Selection of effective therapies using three-dimensional *in vitro* modeling of chondrosarcoma, *Front. Mol. Biosci.* 7 (2020) 566291, <https://doi.org/10.3389/fmolb.2020.566291>.
- [136] D.H. Hamdi, S. Barbieri, F. Chevalier, J.E. Groetz, F. Legendre, M. Demoor, P. Galera, J.L. Lefaix, Y. Saintigny, In vitro engineering of human 3D chondrosarcoma: a preclinical model relevant for investigations of radiation quality impact, *BMC Cancer* 15 (2015) 579, <https://doi.org/10.1186/s12885-015-1590-5>.
- [137] D. Vautier, J. Hemmerlé, C. Vodouhe, G. Koenig, L. Richert, C. Picart, J.C. Voegel, C. Debry, J. Chluba, J. Ogier, 3-D surface charges modulate protrusive and contractile contacts of chondrosarcoma cells, *Cell Motil Cytoskeleton* 56 (2003) 147–158, <https://doi.org/10.1002/cm.10140>.
- [138] M. Minopoli, S. Sarno, G. Di Carluccio, R. Azzaro, S. Costantini, F. Fazioli, M. Gallo, G. Apice, L. Cannella, D. Rea, M.P. Stoppelli, D. Boraschi, A. Budillon, K. Scotlandi, A. De Chiara, M.V. Carriero, Inhibiting monocyte recruitment to prevent the pro-tumoral activity of tumor-associated macrophages in chondrosarcoma, *Cells* 9 (2020) 1062, <https://doi.org/10.3390/cells9041062>.
- [139] M.V. Carriero, K. Bifulco, M. Minopoli, L. Lista, O. Maglio, L. Mele, G. Di Carluccio, M. De Rosa, V. Pavone, UPARANT: a urokinase receptor-derived peptide inhibitor of VEGF-driven angiogenesis with enhanced stability and in vitro and in vivo potency, *Mol. Cancer Ther.* 13 (2014) 1092–1104, <https://doi.org/10.1158/1535-7163.MCT-13-0949>.
- [140] V.A. Parfenov, V.A. Mironov, K.A. van Kampen, P.A. Karalkin, E.V. Koudan, F.D. Pereira, S.V. Petrov, E.K. Nezhurina, O.F. Petrov, M.I. Myasnikov, F.X. Walboomers, H. Engelkamp, P. Christianen, Y.D. Khesuani, L. Moroni, C. Mota, Scaffold-free and label-free biofabrication technology using levitational assembly in a high magnetic field, *Biofabrication* 12 (2020) 045022, <https://doi.org/10.1088/1758-5090/ab7554>.